In-cell recordings by extracellular microelectrodes

Aviad Hai[1], Joseph Shappir[2] & Micha E Spira[1]

Current extracellular multisite recordings suffer from low signal-to-noise ratio, limiting the monitoring to action potentials, and preclude detection of subthreshold synaptic potentials. Here we report an approach to induce *Aplysia californica* neurons to actively engulf protruding microelectrodes, providing 'in-cell recordings' of subthreshold synaptic and action potentials with signal-to-noise ratio that matches that of conventional intracellular recordings. Implementation of this approach may open new vistas in neuroscience and biomedical applications.

Microelectrode arrays are increasingly used for recording in parallel electrical activity from many excitable cells for days and months[1–6]. The devices used for both *in vitro* and *in vivo* recordings have common advantages of recording extracellularly without mechanically damaging the cell's plasma membrane. The main disadvantage of extracellular electrodes is their very low signal-to-noise ratio. Therefore, the use of extracellular electrodes is limited in most studies to recording action potentials[3]. Single excitatory or inhibitory subthreshold synaptic potentials or membrane oscillations cannot be detected by currently used extracellular electrodes. These limitations complicate the analysis of neuronal networks in culture or *in vivo*.

Here we describe an approach in which an extracellular multielectrode array system enables 'in-cell recording' of subthreshold synaptic and action potentials from individual neurons with a signal-to-noise ratio that matches that of conventional intracellular recordings. We refer to the method as in-cell recording by extracellular electrodes, to differentiate it from intracellular recording in which the electrode tip is physically forced to form direct Ohmic contact with the cytosol (the sharp- and whole-cell patch electrode configurations[7]). Key to the multielectrode array in-cell recording approach are: (i) activation of phagocytotic-like mechanisms by which the cultured cells actively engulf gold microelectrodes in the form of microspines that protrude from a flat substrate[8,9] (**Fig. 1a–d**); (ii) generation of high-seal resistance between the cell's membrane and the engulfed spine electrodes[9]; and (iii) localization of ionic channels (Ohmic conductance) in the plasma membrane that faces the gold-spine microelectrodes.

Using ultrastructural and confocal imaging methods we had recently reported that culturing *Aplysia* neurons and different mammalian cell lines (CHO, 3T3, H9C2 and PC12) on matrices of micrometer-sized protruding gold-spines functionalized by a peptide with multiple Arg-Gly-Asp (RGD) repeats greatly improves the physical interface between the cell's plasma membrane and the substratum[8,9]. This peptide, named engulfment-promoting peptide (EPP[9]), facilitates the engulfment of the gold spines.

We grew buccal neurons isolated from *Aplysia*[10] on an array of 62 gold-spine, EPP-functionalized electrodes with interspine intervals of 14 µm (**Fig. 1e**). We carefully impaled one of the neurons by a sharp glass microelectrode for both current injection and voltage recordings (**Fig. 1f**), ensuring that impaling did not exert mechanical pressure that compressed the neuron against the substrate. We collected recordings from the glass microelectrode

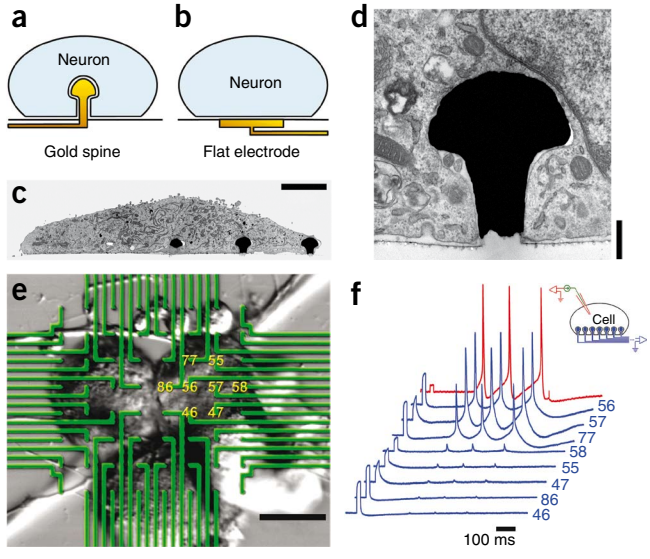

Figure 1 | The structural configuration of a neuron engulfing a functionalized gold-spine electrode and the ensuing electrical coupling. (**a**,**b**) Schematic representations of a neuron engulfing a gold-spine electrode (**a**) and a neuron on a flat electrode (**b**). (**c**) Electron micrograph depicting a cross-section through a PC12 cell engulfing three functionalized gold spines. The gold spine in the center of the image was transected only through the head, and the other two spines were transected along the spine's head and stalk. (**d**) Electron micrograph of a gold spine engulfed by a PC12 cell. (**e**) Confocal microscopy image of three *Aplysia* neurons cultured on a multi–gold spine electrode array. The conducting lines are depicted in green. Scale bars, 5 µm (**c**); 500 nm (**d**); and 50 µm (**e**). (**f**) Simultaneous action potential recordings (blue) from 8 gold-spine electrodes (indicated by numbers in **e**) in response to intracellular stimulation of the neuron by a conventional sharp microelectrode (red). Each trace depicts initially a 5 mV, 20 ms calibration pulse and then, after a delay, three action potentials. Inset, schematic of the experimental setup.

[1]Department of Neurobiology, Life Science Institute and [2]School of Engineering, the Hebrew University of Jerusalem, Jerusalem, Israel. Correspondence should be addressed to M.E.S. (spira@cc.huji.ac.il).

RECEIVED 31 AUGUST 2009; ACCEPTED 13 DECEMBER 2009; PUBLISHED ONLINE 31 JANUARY 2010; DOI:10.1038/NMETH.1420

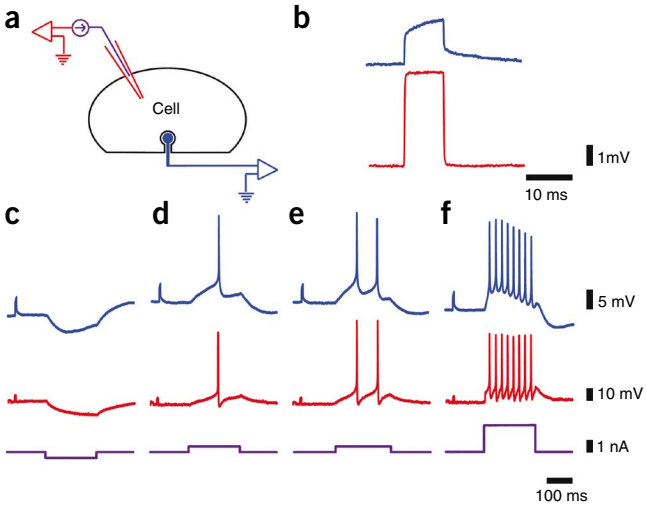

Figure 2 | 'In-cell recordings' by an extracellular gold-spine electrode. (**a**) Schematic presentation of the experimental setup. A neuron engulfing a single gold-spine electrode was penetrated by a sharp microelectrode that was used for both current injection (purple) and voltage recording (red). (**b**) A 10 ms 5 mV square calibration pulse applied to the bathing solution recorded by the intracellular microelectrode (red) and a functionalized gold-spine electrode (FGSE) (blue). (**c**) A hyperpolarizing square current pulse was delivered by the intracellular microelectrode (purple), generated hyperpolarization of the neuron (red) as recorded by the FGSE (blue). (**d**–**f**) Depolarizing currents with increasing amplitudes (purple) delivered by the sharp intracellular microelectrode, generated a single or trains of action potentials of ~50 mV (red, recorded intracellularly) and ~25 mV action potentials (blue, recorded by the FGSE).

with a direct current (DC) amplifier. Concomitantly, we collected recordings from the 62 chemically functionalized gold-spine electrodes (FGSEs) using the Multichannel Systems alternating current (AC) amplifier (MEA-1060-Inv-BC), with frequency limits of 1–10,000 Hz and a gain of 110–1,100.

We delivered a calibration voltage square pulse to the bath solution. Comparison of the shapes and amplitudes of the calibration pulses recorded by the DC–coupled intracellular glass microelectrode and the FGSEs that were amplified by an AC amplifier (**Fig. 1f**) revealed that the impedances of the FGSEs were not identical to each other, and thus altered the shape and amplitude of the calibration pulses in different ways. These alterations were due to the high impedance ionic bilayer formed at the interface of the gold-electrode surface and the bathing solution[11]. We suspect the variability in the electrical properties of the individual FGSEs occurred because we fabricated the devices in our laboratory and could not reach homogeneous fabrication standards. Using conventional capacitance compensation methods, the frequency response of the individual FGSEs can be corrected (**Supplementary Fig. 1**).

Depolarization of the neuron by intracellular current injection generated a train of three action potentials recorded by the intracellular glass microelectrode (**Fig. 1f**). These action potentials were concomitantly recorded by 8 FGSEs that we visually identified to reside under the stimulated neuron. The amplitude of the 'raw' action potentials recorded by the different FGSEs was 0.1–25 mV (using the raw calibration pulses; **Fig. 1f**) reflecting the extent of coupling between the neuron and individual FGSEs (**Supplementary Fig. 1**).

To analyze the quality of the recording by the FGSE, we first examined the recordings from a single FGSE (**Fig. 2**). A 200 ms hyperpolarizing square current pulse of ~0.5 nA delivered intracellularly to the neuron generated a ~10 mV membrane hyperpolarization with a characteristic neuronal membrane time constant (**Fig. 2c**). This was recorded by the AC-coupled FGSE as a filtered hyperpolarization with maximal amplitude (as estimated by the raw calibration pulse) of ~5 mV (**Fig. 2c**). Conversely, a 200 ms, ~0.5 nA depolarizing square current pulse generated an intracellularly recorded action potential (50 mV) riding on a membrane depolarization (**Fig. 2d**). Concomitantly, the AC-coupled FGSE recorded a single action potential (with an estimated amplitude of

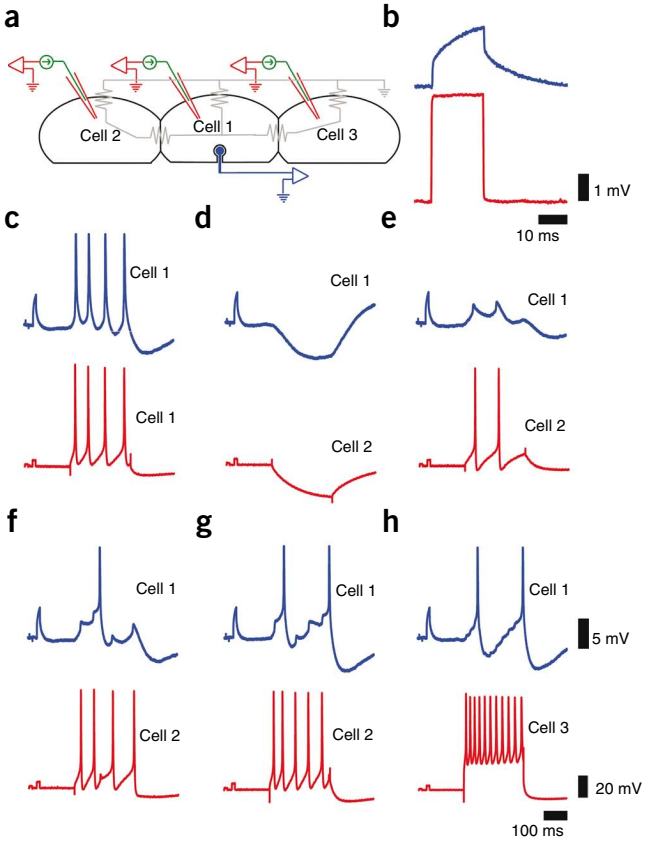

Figure 3 | Synaptic potentials and action potentials recorded by extracellular functionalized gold-spine electrodes (FGSEs). (**a**) Experimental setup: three cells were cultured on the multi-FGSE array. A single glass microelectrode was used for both intracellular stimulation and recordings. (**b**) A calibration pulse of 5 mV, 20 ms as detected by the intracellular microelectrode (red) and a FGSE (blue). (**c**) Depolarization of neuron 1 generated a train of action potentials recorded by the intracellular electrode (red) and the FGSE (blue). (**d**) The intracellular electrode was moved into neuron 2. Hyperpolarization of neuron 2 generated hyperpolarization of neurons 2 and 1. (**e**) Depolarization of neuron 2 generated two action potentials and elicited two electrical EPSPs riding on the depolarizing pulse (blue) in neuron 1. (**f**–**g**) Increasing the strength of the intracellular stimulation of neuron 2 generated trains of 4 (**f**) and 5 (**g**) action potentials in neuron 2 leading to summation of the EPSPs in neuron 1, to fire one (**f**) and two (**g**) action potentials as monitored by the gold spine electrode from neuron 1. (**h**) The intracellular electrode was moved into neuron 3. Action potentials in cell 3 (red) also generated EPSPs, which summed to generate action potentials in cell 1.

25 mV) riding on the depolarizing potential (**Fig. 2d**). Lengthening the depolarizing pulse to 220 ms triggered two action potentials (**Fig. 2e**), and increasing the current injection to ~2 nA generated a train of action potentials recorded by the intracellular glass microelectrode and the FGSE (**Fig. 2f**).

Next we recorded excitatory postsynaptic potentials (EPSPs) from three buccal neurons grown on a multi-FGSE device (**Fig. 3**). Depolarization of cell 1 elicited trains of action potentials recorded by the sharp intracellular microelectrode and the FGSEs (**Fig. 3c**). Moving the intracellular microelectrode to cell 2 while recording the responses from cell 1 by the FGSEs revealed that the two cells were electrically coupled. Thus, hyperpolarizing pulses delivered by the intracellular electrode to cell 2 generated hyperpolarization of cells 2 and 1 (**Fig. 3d**). Action potentials generated in cell 2 were accompanied by electrical EPSPs recorded in cell 1 (**Fig. 3e**). When we delivered a stronger depolarizing pulse to cell 2, the electrical EPSPs summed to fire an action potential in cell 1 (**Fig. 3f**,**g**). Transferring the intracellular electrode to cell 3 revealed that a train of action potentials generated in cell 3 evoked summating EPSPs recorded by the FGSE in cell 1 (**Fig. 3h**). Consistent with the extracellular position of the FGSE in respect to the neurons, the stimulation and recording sessions above lasted as long as 2 h.

These experiments demonstrate that neurons interfaced with FGSEs formed an unexpected junction that supported high electrical coupling. Coupling between the neurons and the FGSEs was voltage-independent, indicating that the conducting elements in the junctional membranes (probably ionic channels) were voltage-independent. But what accounts for the efficient coupling between the neurons and the engulfed FGSE?

Prior experimental and theoretical considerations revealed that the limiting factors for effective electrical coupling between neurons and flat extracellular sensing pads of microfabricated electrical devices is the seal resistance (R_{seal})[12,13] and the conductance of the patch of plasma membrane across it (the junctional membrane, g_j) (for a review, see ref. 3). Our ultrastructural studies[8,9] revealed that cells tightly engulfed the FGSE while the electrode remained extracellular. These ultrastructural studies enabled us to estimate R_{seal}[9], but we could not predict the high electrical coupling between the neurons and the FGSEs.

To understand the unprecedented electrical coupling between the neurons and the electrodes, we examined an analog electrical circuit of the neuron-FGSE configuration and developed a simple model of the coupling (**Supplementary Note**). The electrical model suggested that to obtain the high coupling, the junctional membrane resistance between the FGSE and the cell interior had to be substantially lower than the nonjunctional membrane resistivity. If we assume that the junctional membrane conductance is increased by recruitment of voltage independent ionic channels such as potassium channels with channel conductance of 10 to 100 picosiemens, then ~10–100 such channels have to concentrate within the confined area of the junctional membrane. This would imply a density of ~ 0.5–10 channels μm^{-2}. Such channel density has been experimentally documented[14]. Lowering the junctional conductance by two orders of magnitude resulted in a substantially lower coupling coefficient (**Supplementary Note**).

It is important to recall that the coupling between the cells and the FGSEs depends on the value of the seal resistance. The physical principles that enable the in-cell recording configuration are well established and have been described in earlier studies[12,13]. In fact, the principles are identical to those of the perforated patch electrode configuration[15].

As we established that several vertebrate cell lines engulf the FGSE and form tight contact[9], it is reasonable to assume that the in-cell recording approach can be applied to other excitable cell types *in vitro* and possibly even *in vivo*.

METHODS

Methods and any associated references are available in the online version of the paper at http://www.nature.com/naturemethods/.

Note: Supplementary information is available on the Nature Methods website.

ACKNOWLEDGMENTS

This work was supported by the "Brain Storm" project (EU P7 215486 STREP). Parts of the study were carried out at the Charles E. Smith and Professor Elkes Laboratory for Collaborative Research in Psychobiology. The fabrication of the gold spines electrode was carried at the Harvey M. Kruger Family center for Nanoscience and Nanotechnology. We thank N. Mazurski for expertise in device fabrication. M.E.S. is the Levi DeViali Professor in neurobiology. A.H. was partially supported by a scholarship from The Israel Council for Higher Education.

AUTHOR CONTRIBUTIONS

A.H. and M.E.S. designed and conducted all experiments, analyzed the data and wrote the manuscript. J.S. designed fabrication processes and took part in the analysis of the data.

COMPETING INTERESTS STATEMENT

The authors declare no competing financial interests.

Published online at http://www.nature.com/naturemethods/.
Reprints and permissions information is available online at http://npg.nature.com/reprintsandpermissions/.

1. Schwartz, A.B. *Annu. Rev. Neurosci.* **27**, 487–507 (2004).
2. Nicolelis, M.A. & Lebedev, M.A. *Nat. Rev. Neurosci.* **10**, 530–540 (2009).
3. Fromherz, P. In *Neuroelectronic interfacing: semiconductor chips with ion channels, nerve cells, and brain* (ed., Waser, P.) (Wiley-VCH, 2003).
4. Hochberg, L.R. *et al. Nature* **442**, 164–171 (2006).
5. Velliste, M., Perel, S., Spalding, M.C., Whitford, A.S. & Schwartz, A.B. *Nature* **453**, 1098–1101 (2008).
6. Berdondini, L. *et al. Lab Chip* **9**, 2644–2651 (2009).
7. Sakmann, B. & Neher, E. *Annu. Rev. Physiol.* **46**, 455–472 (1984).
8. Spira, M.E. *et al. Solid-State Sensors, Actuators and Microsystems Conf.* (doi: 10.1109/SENSOR.2007.4300363) 1247–1250 (2007).
9. Hai, A. *et al. J. R. Soc. Interface* **6**, 1153–1165 (2009).
10. Bailey, C.H. & Kandel, E.R. *Prog. Brain Res.* **169**, 179–198 (2008).
11. Mortari, A., Maaroof, A., Martin, D. & Cortie, M.B. *Sens. Actuators B Chem.* **123**, 262–268 (2007).
12. Jenkner, M. & Fromherz, P. *Phys. Rev. Lett.* **79**, 4705–4708 (1997).
13. Cohen, A., Shappir, J., Yitzchaik, S. & Spira, M.E. *Biosens. Bioelectron.* **23**, 811–819 (2008).
14. Hille, B. *Ion Channels of Excitable Membranes* (Sinauer, 2001).
15. Akaike, N. & Harata, N. *Jpn. J. Physiol.* **44**, 433–473 (1994).

ONLINE METHODS

Fabrication of gold-spine multielectrode arrays. Multi–gold spine electrode arrays for electrical measurements were prepared on glass wafers as previously described[9]. Briefly, wafers were coated with a titanium (10–15 nm) and gold (45–65 nm) layer by evaporation, spin-coated with photoresist S-1813 (4,000 r.p.m.), baked for 30 min (90 °C), after which a first photolithographic process was performed followed by Au/Ti wet etch to define the multielectrode array. Next a second lithographic step with thick photoresist was performed to open holes for the deposition of the gold-spine stalks. Gold-spines were grown by electroplating. Next, a layer of silicon oxide (~3,000 Angstrom) was deposited by chemical vapor deposition processing. A third layer of photoresist was then applied. A third lithographic step was used to expose the contact pads and the heads of the gold spines followed by wet oxide etch to selectively remove the oxide from the contact pads and the gold spine heads. Wafers were then sawed and underwent manual bonding to 62-pad printed circuit boards to which 21 mm glass rings were attached to create a bath for the culture medium.

Surface functionalization. The cysteine-terminated EPP[8,9], CKKKKKKKKKPRGDMPRGDMPRGDMPRGDM (molecular weight, 3,630 g mol^{-1}) with several RGD repeats and a decalysine spacer was functionalized as follows: gold-spines surface was functionalized by direct application of the peptide onto the surface (1 mM in phosphate buffer saline at room temperature (20–25 °C)). The glass surface between gold-spines was functionalized using 3-aminopropyltriethoxysilane (APTMS; Aldrich; 1% in MeOH, 10 min at room temperature) to introduce terminal amine groups to the glass surface. The devices were then washed with MeOH to remove uncoupled APTMS. The protein immobilization linker 4-maleimidobutyric acid sulfo-*N*-succinimidyl ester (sGMBS; Sigma; 0.5% in PBS) was then applied to the surface and washed with PBS (pH 7.6) after 40 min at room temperature. EPP peptide was then applied to the surface and left for 24 h, during which time the cysteinic thiol residue reacted with the maleimido part of the anchored linker. Samples were then washed with PBS.

Cell culture. Neurons from the buccal ganglia of *Aplysia californica* were isolated and maintained in culture as previously described[16]. Briefly, juvenile *Aplysia* (1–10 g) supplied from the University of Miami, National Resource for *Aplysia*, were anesthetized by injecting isotonic $MgCl_2$ solution (380 mM) into the body cavity. Ganglia were dissected and incubated in L-15 supplemented for marine species (ms L-15) containing 1% protease (type IX; Sigma-Aldrich) at 34 °C for 1.5–2.5 h. After the protease treatment, the ganglia were desheathed. Individual neurons were manually pulled out along with their original axons with the aid of a sharp glass microelectrode and plated on the devices. Plated *Aplysia* neurons survive in culture for over a month, extend neurites and form chemical and electrical synapses[10]. For this study, neurons plated on the FGSE devices were cultured for 48—96 h at 24 °C and then used for the electrophysiological experiments. For this study, the FGSE devices were used once.

Electrophysiology. Conventional intracellular recording and stimulation of cultured *Aplysia* neurons were used as previously described[9]. The microelectrodes were pulled from 1.5 mm outer diameter, 1.02 mm inner diameter borosilicate glass tubes with filaments and filled with 2 M KCl. Electrode resistance ranged between 4 and 10 MΩ. For intracellular recording and stimulation, the microelectrode tip was inserted into the cell body.

Recordings were made from the 62 chemically functionalized gold-spine electrodes (FGSEs) using the Multichannel Systems AC amplifier (MEA-1060-Inv-BC), with frequency limits of 1–10,000 Hz and a gain of 110–1,100. The data shown are of raw, unprocessed recordings.

16. Spira, M.E. *et al. J. Neurosci. Methods* **69**, 91–102 (1996).

Supplementary Figure 1

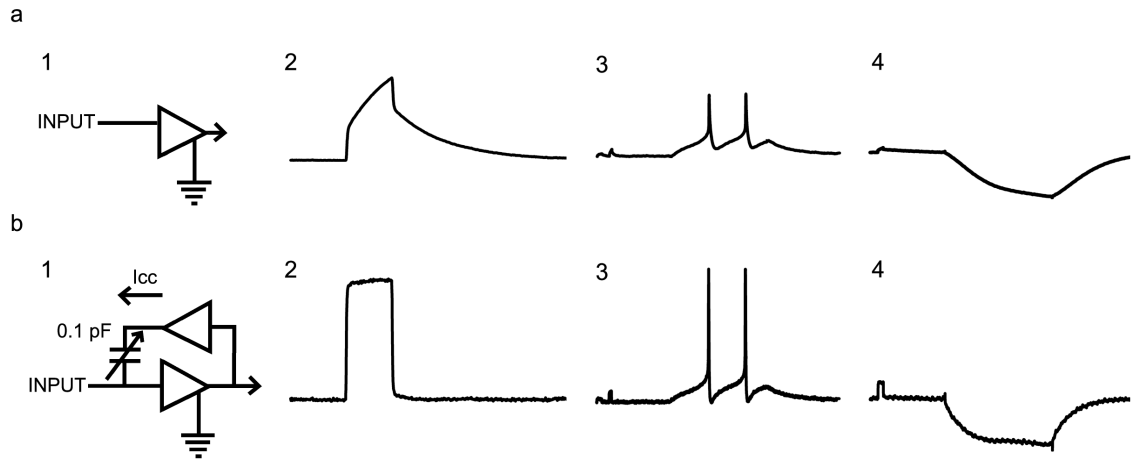

Supplementary Fig. 1. Deconvolution of recorded signal by capacitance compensation. (a) The raw signals recorded by the FGSE are distorted as a result of the electrode impedance and the parasitic capacitance of the recording setup. **(a1)** Schematic representation of the amplifier. **(a2)** A 5 mV, 10 ms calibration square pulse as revealed by recording from the FGSE. **(a3)** Recording of two action potentials riding on a depolarizing pulse delivered intracellularly to the neuron and recorded by the FGSE. The voltage calibration pulse is shown at the onset of the traces. **(a4)** A hyperpolarizing pulse as recorded by the FGSE. **(b)** Capacitance compensation circuit consisting of an additional amplifier and adjustable capacitor (b1) compensates for the stray capacitance by injecting an opposite current (I_{cc}) through the amplifier input and de-convolutes the signal, restoring its original shape. **(b2)** The deconvoluted calibration pulse of (a2). **(b3)** The deconvoluted action potentials shown in (a3), and **(b4)** the deconvoluted form of (a4). Values used for the adjustable capacitor and resistor were 0.1 pF and 1000 GΩ, respectively.

Deconvolution of recorded signal by capacitance compensation

Whereas the signal-to-noise ratio of the recording by the FGSEs depicted in the experiments of figure 1, 2 and 3 are similar to those of the intracellular recordings, the FGSE impedance, and the recording setup altered the shape and attenuated the amplitude of the potentials. These alterations can be corrected by introducing a conventional negative capacitance compensation circuit[1,2]. Supplemental figure 1 simulates the output waveforms of a 5mV, 10ms calibration square pulse, and an action potential without (upper row) and with a capacity compensation circuit (lower row). The values of the negative capacitance circuit are given in the illustration.

Supplementary Note

Computer simulation of the coupling between a neuron and an extracellular functionalized gold-spine electrode

To provide an explanation that could account for the unprecedented electrical coupling between the neuron and the functionalized gold spine electrode (FGSE) we examined an analog electrical circuit of the neuron-FGSE configuration (Fig. A). The majority of the parameters used to assess the electrical coupling were obtained from direct measurements, or by calculations of the physical parameters that fit the specific geometry and dimensions of the cell-device interface (the calculations and parameters used are detailed below). Briefly, the values used to generate the default simulation (in which the junctional membrane conductance is not elevated) are: **(A) neuronal membrane parameters:** the non-junctional membrane resistance R_{nj}- 25 MΩ. The junctional membrane resistance is R_j-100 GΩ. The non junctional membrane capacitance (C_m) is taken as 600 pF. The calculated junctional membrane capacity (C_j)- 0.1 pF. **(B) FGSE and amplifier parameters:** The FGSE to solution resistance (R_{FGSE}) is 1000 GΩ. The capacity of the gold

spine electrode in solution is 7 pF. The amplifier input capacitance 8 pF. **(C) The seal resistance formed between the cell's membrane, and ground** is 100 MΩ.

Using these values we found that the coupling between the neuron and the FGSE is practically zero (Fig. A(a)). To generate a coupling coefficient that corresponds to the experimental results, R_j had to be lowered from an estimated value of 100 GΩ to 100 MΩ (Fig. A(c)). Assuming that the junctional membrane conductance is increased by recruitment of voltage independent ionic channels such as potassium channels with channel conductance of 10 to 100 pS, then, ~10-100 such channels have to concentrate within the confined area of the junctional membrane. This would imply a density of approximately 0.5 to 10 channels/μm^2. It is interesting to note that such channel density was experimentally documented in a number of cell types[14]. Lowering R_j by two orders of magnitude results in a significantly lower coupling coefficient (Fig A(d)). A relative large increase in in respect to the input resistance could theoretically alter the electrical properties of the neurons. We therefore measured the passive and active membrane properties, synaptic transmission and growth pattern of neurons grown on matrices of FGSE and found that neurons maintained normal properties (not shown). This implies that the simulated increase in g_j is minute in respect to the neuron's input resistance.

It is important to recall that the coupling between the cells and the FGSE depends on the value of the seal resistance. And reduction of the seal resistance to values below 100 MΩ reduces the coupling coefficient (generated by the parameters of the simulation in Fig A(c)) by three orders of magnitudes.

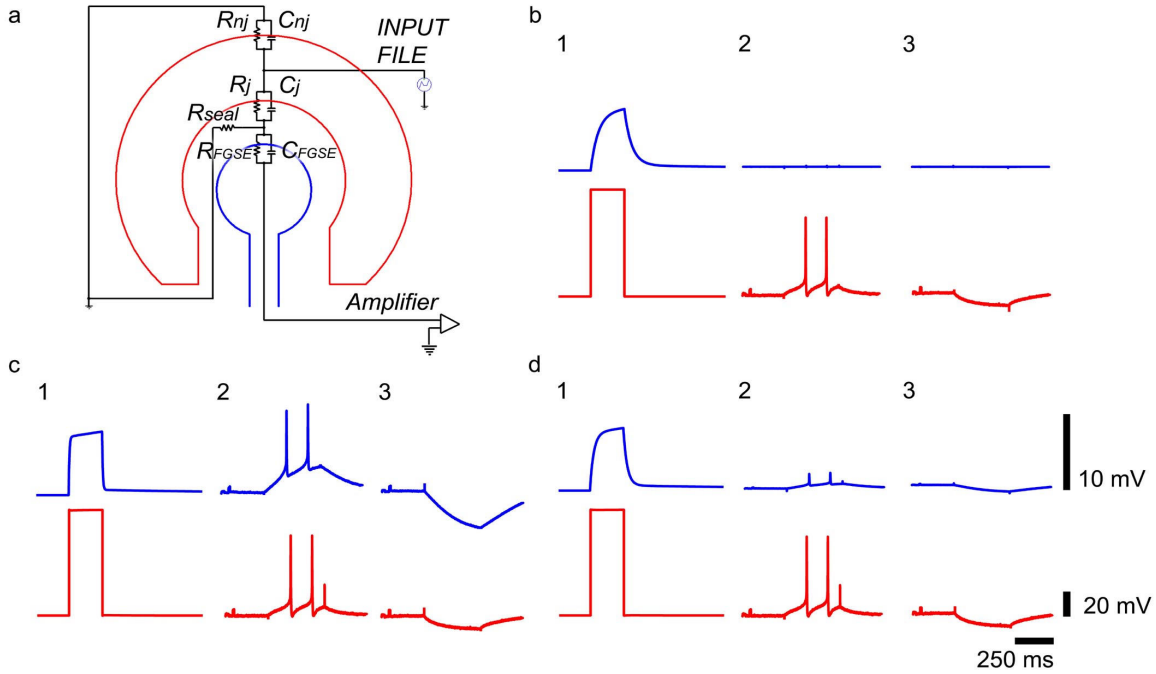

Fig. A. Computer simulation of the coupling between a neuron and an extracellular functionalized gold-spine electrode using a minimal equivalent electrical circuit. (**a)** The equivalent circuit used for the simulation. (**b – d),** Simulated results. The components of the analog electrical circuit and default values are described in the text and the supplemental material. For the simulation a calibration pulse of 5 mV and 20 ms (1), two action potentials (2) and a hyperpolarizing pulse (3) were fed into the simulated neuron (red traces). Recordings were made from the spine (blue). The simulation reveals that using the default values no coupling between the cell and the FGSE can be detected (**b)**. Lowering the junctional membrane resistance from 100 GΩ to 100 MΩ (while maintaining all other default values) qualitatively generated equivalent coupling to those observed in the experiments (**c)**. A smaller decrease of the junctional membrane resistance (to 1 GΩ) generates a significantly smaller coupling value (**d**). The simulation thus supports the view that the level of coupling depends on the junctional membrane resistance given that the value of R_{seal} was correctly estimated.

In the following we specify in detail the parameters and values used in the electrical model.

1. neuronal membrane parameters

1.1 The non-junctional membrane resistance (R_{nj}) was measured in a large number of neurons. The input resistance (R_{in}) ranges between 15-30 MΩ. We selected to use a value of 25 MΩ in accordance with the experimentally R_{in} . It should be noted that the small surface area of the junctional membrane renders R_{nj} and R_{in} to be equal.

1.2 For the estimation of the **junctional membrane resistance (R_j)** we first estimated the surface area of the functionalized gold-spine electrode (FGSE) approximated as a cylinder-shaped stalk and a sphere-shaped head:

$$A_{FGSE} = A_{stalk} + A_{head} \qquad (1.2.1)$$

Where:

$$A_{stalk} = 2\pi \cdot r_{stalk} \cdot h_{stalk} \qquad (1.2.2)$$

And:

$$A_{head} = 4\pi \cdot r_{head}^{\ 2} \qquad (1.2.3)$$

Estimating r_{stalk}, r_{head} and h_{stalk} to be 0.5, 1 and 0.5 µm, respectively, we get:

$$A_{FGSE} \approx 14\mu m^2 \qquad (1.2.4)$$

Next, we multiplied the total input resistance (R_{in}) with the ratio between the surface area of the neuron (A_{neuron}) and the surface area of the GS (A_{GS}). Assuming the cell consists of a sphere with radius (r_{soma}) of 50 µm and a cylindrical axon with a radius (r_{axon}) of 5 µm and a length (l) of 500 µm, we get:

$$\begin{aligned} A_{neuron} &= A_{soma} + A_{axon} \\ &= 4\pi \cdot r_{soma}^{\ 2} + 2\pi \cdot r_{axon} \cdot l \approx 6 \cdot 10^4 \mu m^2 \end{aligned} \qquad (1.2.5)$$

and thus:

$$R_j = R_{in} \cdot \frac{A_{neuron}}{A_{FGSE}} = 25 \cdot 10^6 \cdot \frac{6 \cdot 10^4}{14} \approx 100G\Omega \qquad (1.2.6)$$

1.3 The non-junctional membrane capacitance C_{nj} equals the total membrane capacitance C_m (according to the same considerations of area ratio, see 1.1) and was set to 600 pF as measured previously in our laboratory[3]

1.4 The estimated junctional membrane capacitance (C_j) is calculated as the total membrane capacitance (C_m) divided by the ratio between the surface area of the cell (A_{neuron}) and the surface area of the gold spine (A_{FGSE}):

$$C_j = C_m \frac{A_{FGSE}}{A_{cell}} = 600 \cdot 10^{-12} \cdot \frac{14}{6 \cdot 10^4} \approx 0.1pF \qquad (1.4.1)$$

2. FGSE and amplifier parameters

2.1 The FGSE resistance (R_{FGSE}) in solution was estimated to be 1000 GΩ in accordance with the measured resistance of gold electrodes in physiological solution[4] normalized by the FGSE surface area (A_{FGSE}) – see section 1.2.

2.2 The capacity of the FGSE in solution is estimated by taking the specific capacity of gold electrical double layer (C_{EDL}) to be ~50 μF/cm^2 (see[5]) multiplied by the surface area of the FGSE (A_{FGSE}):

$$C_{FGSE} = C_{EDL} \cdot A_{FGSE} = 50 \cdot 10^{-6} \cdot 14 \cdot 10^{-8} = 7\,pF \qquad (2.2.1)$$

2.3 The amplifier input capacitance is 8 pF (Multichannel systems, Rutlingen, Germany).

3. The seal resistance (R_{seal}) formed between the cell's membrane, and grounded solution is taken as ~100 MΩ as was previously estimated[6].

1. McGillivray, R. & Wald, R. Dual-path capacitance compensation network for microelectrode recordings. *Am J Physiol* **238**, H930-1 (1980).
2. Wilson, C. J. & Park, M. R. Capacitance compensation and bridge balance adjustment in intracellular recording from dendritic neurons. *J Neurosci Methods* **27**, 51-75 (1989).
3. Ashery, U., Penner, R. & Spira, M. E. Acceleration of membrane recycling by axotomy of cultured aplysia neurons. *Neuron* **16**, 641-51 (1996).
4. McAdams, E. T., Jossinet, J., Subramanian, R. & McCauley, R. G. Characterization of gold electrodes in phosphate buffered saline solution by impedance and noise measurements for biological applications. *Conf Proc IEEE Eng Med Biol Soc* **1**, 4594-7 (2006).
5. Mirsky, V. M., Riepl, M. & Wolfbeis, O. S. Capacitive monitoring of protein immobilization and antigen-antibody reactions on monomolecular alkylthiol films on gold electrodes. *Biosens Bioelectron* **12**, 977-89 (1997).
6. Hai, A. et al. Spine-shaped gold protrusions improve the adherence and electrical coupling of neurons with the surface of micro-electronic devices. *J R Soc Interface* **6**, 1153-65 (2009).